

Nitrogen-Rich and Fire-Resistant Carbon Aerogels for the Removal of Oil Contaminants from Water

Yu Yang,[†] Zhen Tong,[†] To Ngai,^{*,‡} and Chaoyang Wang^{*,†}

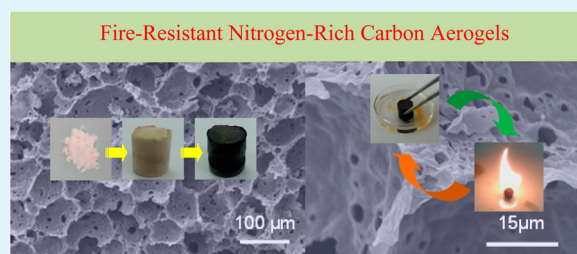
[†]Research Institute of Materials Science, South China University of Technology, Guangzhou 510640, China

[‡]Department of Chemistry, The Chinese University of Hong Kong, Shatin N.T., Hong Kong

S Supporting Information

ABSTRACT: Effective removal of crude oils, petroleum products, organic solvents, and dyes from water is of significance in oceanography, environmental protection, and industrial production. Various techniques including physical and chemical absorption have been developed, but they suffer from problems such as low separation selectivity, a complicated and lengthy process, as well as high costs for reagents and devices. We present here a new material, termed nitrogen-rich carbon aerogels (NRC aerogels,) with highly porous structure and nitrogen-rich surfaces, exhibiting highly efficient separation of specific substances such as oils and organic pollutants. More importantly, we demonstrate that the fabricated NRC aerogels can also collect micrometer-sized oil droplets from an oil-water mixture with high efficiency that is well beyond what can be achieved by most existing separation methods, but is extremely important in practical marine oil-spill recovery because a certain amount of oils often shears into many micrometer-sized oil droplets by the sea wave, resulting in enormous potential destruction to marine ecosystem if not properly collected. Furthermore, our fabricated material can be used like a recyclable container for oils and chemicals cleanup because the oil/chemical-absorbed NRC aerogels can be readily cleaned for reuse by direct combustion in air because of their excellent hydrophobicity and fire-resistant property. We demonstrate that they keep 61.2% absorption capacity even after 100 absorption/combustion cycles, which thus has the highest recyclability of the reported carbon aerogels. All these features make these fabricated NRC aerogels suitable for a wide range of applications in water purification and treatment.

KEYWORDS: adsorbents, carbon aerogels, Pickering emulsions, template synthesis, fire-resistance, environmental chemistry



1. INTRODUCTION

Effective removal of oil from water is of significant in oceanography and environmental protection. With the development of international trade and marine petroleum exploitation, oil spill accidents are of common occurrence, doing catastrophic damage to the ocean and coast near the oil leakage area.^{1–11} Materials that can eliminate these oily contaminants are urgently needed. Hydrophobic porous aerogels have been introduced as physical adsorbents for oil-spill cleanup, because of their low density, hydrophobicity, high porosity, chemical inertness, and large specific surface area.^{12–18} Until now, various hydrophobic porous aerogels have been successfully synthesized in different methods and exhibit highly efficient absorption of spilled oils, such as carbon nanotube sponges fabricated by chemical vapor deposition (CVD),¹⁹ spongy graphenes synthesized by reducing graphene oxide platelets,^{20,21} hydrophobic porous polymethylsilsesquioxane aerogels created by controlling phase separation in the sol-gel process,²² carbonaceous nanofiber aerogels based on hydrothermal carbonization process,²³ and polyurethane sponges fabricated by solution-immersion processes.²⁴ Other materials based on carbonizable polymer (such as polyurethane²⁵ and resorcinol-formaldehyde²⁶) or biomass (such as bacterial cellulose by Yu's group²⁷ and raw cotton by Zhang's

group²⁸), through the pyrolysis treatment at high temperature, to enhance their hydrophobicity are also widely reported. Moreover, these pyrolyzed carbon aerogels may have excellent fire-resistant properties due to their graphite skeletons, which are generated during the pyrolysis process. When adsorbed by oily ingredients that have a very high boiling point, they cannot be simply regenerated by conventional absorption/distillation cycles. But these fire-resistant aerogels can make a more appropriate choice of absorption/combustion cycles for reuse, vastly broadening their applications. Despite their outstanding potential, several challenges in aerogel synthesis still must be addressed prior to their extensive practical applications, such as complicated and lengthy process, high costs for reagents and devices, poor mechanical stability, and especially their unsatisfactory regeneration and cycling. Furthermore, in practical marine oil-spill recovery, there is a certain amount of oil that is sheared into many micrometer-sized oil droplets by the sea wave and that cannot be effectively absorbed by traditional adsorbents, leading to enormous potential destruction to marine ecosystem.^{1,7} Therefore, considerable efforts

Received: December 12, 2013

Accepted: April 17, 2014

Published: April 17, 2014

should be devoted to exploring a simple and low-cost approach to fabricate robust hydrophobic porous aerogels with excellent recyclability and oil droplet adsorbability.

Recently, a soft-templating approach starting from a high internal phase emulsion (HIPE, a type of emulsion with a volume fraction of the disperse phase higher than 74%) was applied to produce highly porous materials with the simply polymerization of the monomers in the continuous phase,^{29–33} and these HIPE-templated porous aerogels composed of hierarchically porous honeycomb-like framework exhibit excellent mechanical strength.^{33–36} But the stabilization of conventional surfactant-stabilized HIPEs presents a challenge in the formation process of porous polymer materials. Fortunately, Pickering HIPEs, which are solid particle-stabilized HIPEs in the absence of any molecular surfactants, exhibit the excellent stabilization compared with the molecular surfactant-stabilized HIPEs, because of the irreversible adsorption of solid particles with their high attachment energy at the oil/water interface.^{37,38} Therefore, the Pickering HIPE templates can commendably maintain the defined porous structure during the polymerization process as their remarkable stability against droplet coalescence, being ideal templates to prepare porous aerogels with the designed structure. Moreover, specific properties can be easily endowed to the Pickering HIPE-templated aerogels by using functional particles as solid surfactants (such as Fe₃O₄ nanoparticles for magnetic performance,³⁹ graphene oxide nanosheets for electrochemical property⁴⁰ and TiO₂ nanoparticles for catalysis⁴¹) or using some specific monomers in the continuous phase for polymerization (such as poly(*N*-isopropylacrylamide) for thermosensitivity³² and polycyclic polymers for carbonizable property³⁸). Very recently, we have successfully prepared melamine formaldehyde polymer (PMF) aerogels based on lignin particle-stabilized Pickering oil-in-water HIPEs.³² These as-prepared PMF aerogels consist of a well-organized interconnected porous structure, exhibiting excellent adsorption capacity of heavy metal ions from aqueous solutions due to their rich in nitrogen and hydrophilic surfaces. Meanwhile, the inexpensive PMF is a kind of carbonizable polymer with triazine rings in its chains. Inspired by that, herein we promote the synthesis process to further fabricate a nitrogen-rich carbon aerogel (NRC aerogel) by pyrolysis the PMF porous aerogel at a high temperature. The new robust NRC aerogels possess highly porous structure and excellent fire-resistant property as expected, and exhibit as an ideal candidate for highly efficient separation of oils and organic pollutants for their highly hydrophobicity. More importantly, the fabricated NRC aerogels can also collect micrometer-sized oil droplets from an oil-water mixture with high efficiency. Furthermore, they can be used like a recyclable container for oil and chemical clean-up, as the oil/chemical-adsorbed NRC aerogels can be readily cleaned for reuse by direct combustion in the air because of their excellent hydrophobicity and fire-resistant property, exhibiting multifunctional characteristics and potential applications in oil-spill clean-up and industrial oily wastewater treatment.

2. EXPERIMENTAL SECTION

2.1. Materials. Alkaline lignin was produced based on the Kraft pulping process.³⁶ Melamine (Sinopharm Chemical Reagent Co. Ltd., China) was directly used. Toluene and 37.0 wt % formaldehyde aqueous solution were obtained from Guangdong Guangzhou Chemical Factory Co. Ltd., China. Acetic acid (Jiangsu Qiangsheng Chemical Reagent Co. Ltd., China) and triethanolamine (TEA,

Tianjin Fuyu Chemical Reagent Co. Ltd., China) were used to adjust the pH value of solutions. Water used in all experiments was purified by filtration and deionization with a Millipore (MA, USA) purification device with a resistivity larger than 18.0 MΩ cm.

2.2. Preparation of Lignin Particles and MF Prepolymer Monomers (pre-MF). Lignin particles were successfully synthesized as follows: 1 wt % lignin aqueous dispersion was prepared by adding certain amounts of lignin powder to deionized water. Then, concentrated ammonia solution (37 wt %) was added to adjust the pH value of the lignin dispersion, until lignin was totally dissolved. The pH was about 11, and lignin solution was obtained. Finally, the pH value of the lignin solution was adjusted to about 3 by adding HCl (1 M). Lignin particles were produced and dispersed in the solution.

The pre-MF monomer was prepared as follows: formaldehyde aqueous solution (3.5 mL) and melamine (1.75 g) were mixed in a 50 mL two-necked round bottom flask which was connected to a reflux condenser and equipped with stirring rod. The pH value of the solution was then adjusted to about 9.5 by 2.5 mL of triethanolamine under mechanical stirring. The mixture was heated to 60 °C. After 30 min, the MF pre-polymer solution was obtained. The continuous aqueous phase was prepared by mixing certain volume ratio of prepolymer solution and lignin particles dispersion, and the pH was adjusted around 3 by adding HCl (1 M). The concentration of lignin particles was fixed at 1 wt %, and the concentration of the pre-MF in outer aqueous phase was kept at 75% in this work.

2.3. Fabrication of NRC Aerogels. Fifteen milligrams of lignin was added into 1.5 mL of aqueous solution consisting of 0.375 mL of water and 1.125 mL of pre-MF. After the lignin completely dissolved, the pH of the solution was adjusted to 3 by adding HCl (1 M). Lignin particles were formed and dispersed in the solution. Lignin particle-stabilized oil-in-water HIPEs with 85 vol % internal phase fraction are normally prepared by stirring the continuous phase vigorously under continued stirring at 400 rpm while slowly adding 8.5 mL of the toluene droplet phase. Once all of the toluene phase had been added, the mixture was stirred at 1000 rpm for 2 min to allow better homogenization of the HIPE. Subsequently, these lignin particle-stabilized high internal Pickering emulsions were transferred into an oven and polymerized at 70 °C for 4 h. The products were purified with ethanol to remove the internal toluene, and air-dried at room temperature for 24 h to constant weight. The porous PMF aerogels were obtained. The obtained PMF aerogels were transferred into a tubular furnace for pyrolysis under a nitrogen flow. The PMF aerogel precursors were heated to 400, 500, 600, and 700 °C at 5 °C/min and held at these temperatures for 2 h to allow complete pyrolysis, and cooled to 100 °C at 5 °C/min, finally, cooled to room temperature naturally to yield black and ultralight NRC aerogels. The NRC aerogels always referred to the products generated from PMF aerogel pyrolyzed at 700 °C, if there is no special declaration.

2.4. Oil and Micrometer-Sized Oil Droplet Removal Test. First, we measured the absorption capacity of the NRC aerogels for various organic solvents and oils. The oil or organic solvent was poured on the surface of water contained in a beaker. NRC aerogels were forced into the organic liquids for fully absorbed and then picked out for measurements. The NRC aerogels weights before and after absorption were recorded for calculating the values of weight gain.

Numerous micrometer-sized oil droplets were generated by ultrasonically treating the mixture of toluene and deionized water (1:10, toluene:water, by volume). The oil droplets remove test was carried out by forcing the NRC aerogels into the toluene-in-water emulsions. With oscillation at 300 rpm by oscillator for a certain time, the milky emulsions turned to be colorless and transparent.

2.5. Regeneration of NRC Aerogels. The regeneration of oil-adsorbed NRC aerogels includes absorption/distillation and absorption/combustion ways. First, in absorption/distillation cycles, the oil-adsorbed NRC aerogels was regenerated by heat treatment at a certain temperature around boiling point of the oil, and then the dried NRC aerogels were used in the further cycle. For absorption/combustion cycles, the oil-adsorbed NRC aerogels were applied for direct combustion in air, and then the no-oil NRC aerogels were used in

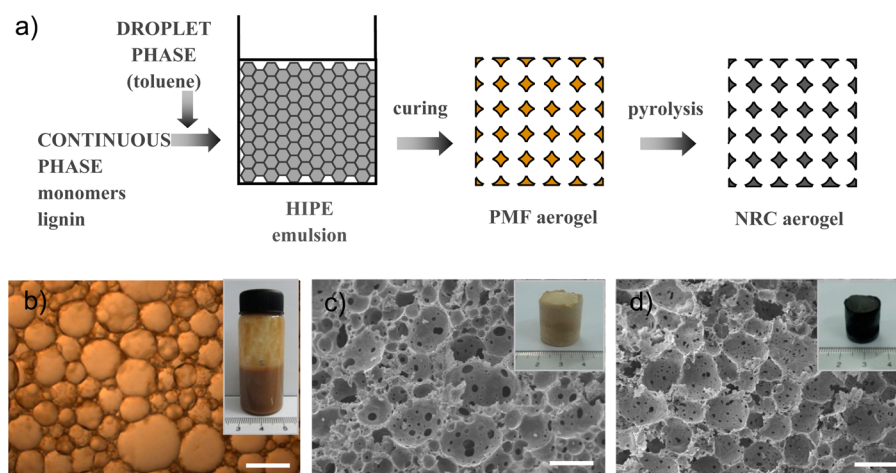


Figure 1. (a) Formation of NRC aerogels by lignin particle-stabilized toluene-in-water Pickering HIPEs polymerization technique. (b) Optical microscope image of lignin particle-stabilized HIPE droplets, with an internal phase fraction of 85%, and the inset is the picture of emulsions. (c) SEM image of PMF aerogel prepared by HIPE of b, and the inset is the picture of the obtained PMF aerogel. (d) SEM image of NRC aerogel based on the PMF aerogel of c, and the inset is the picture of the obtained NRC aerogel. All scale bars present 100 μm .

the next cycle. The weights of NRC aerogels were recorded before and after each cycle to determine the absorption capacity.

2.6. Characterization. Pickering emulsions were observed with a microscope (Carl Zeiss, German). The sample structure was observed by Scanning electron microscopy (SEM) images which were taken with a Zeiss EVO 18 scanning electron microscope equipped with a field emission electron gun, and the amounts of C, N and O were determined by energy-dispersive spectrometer (EDS) at an acceleration voltage of 5 kV. X-ray diffraction (XRD) pattern of the samples was collected by PANalytical X'Pert PRO X-ray diffractometer (Almelo, Netherlands). The Raman spectra were recorded on a spectrometer (JYH800UV) equipped with an optical microscope at room temperature. Fourier transform infrared spectroscopy (FT-IR) was carried out by German Vector-33 IR instrument. TGA was performed using a NETZSCH TG 209 instrument under an air atmosphere and a heating rate of 10 $^{\circ}\text{C min}^{-1}$ from 30 to 800 $^{\circ}\text{C}$. The wetting properties of different samples were evaluated through contact angle tests, which were performed by the CAST2.0 contact angle analysis system at room temperature (OCA20LHT-TEC700-HTFC1500, Dataphysics, Germany).

3. RESULTS AND DISCUSSION

3.1. Preparation and Characterization of NRC Aerogels. A simple and effective method was applied for the fabrication of NRC aerogels with highly porous structure via O/W Pickering HIPE templates. Particularly, as shown in Figure 1, certain amount of toluene was gradually added into an aqueous mixture which composed of lignin particle and MF prepolymer monomers to form a lignin particle-stabilized Pickering HIPE. The optical microscope images of the formulated Pickering HIPEs (Figure 1b) show that the oil droplets are highly packed and deformed, a typical feature of the HIPEs. Therefore, the thickness of the contact domains between the neighboring droplets is thin enough to form pore throats during the polymerization, and it is advantageous to the formation of open-cell porous structure. The average droplet size ranges from 50 to 120 μm and the size distribution of the droplet is quite polydisperse. The small droplets fill in the trigonal region among the big droplets, and template with this honeycomb-like structure is benefit to prepare robust aerogels. Moreover, the lignin-stabilized Pickering HIPEs were remarkable stable against coalescence even after standing for 3 months at room temperature, owing to the nearly irreversible

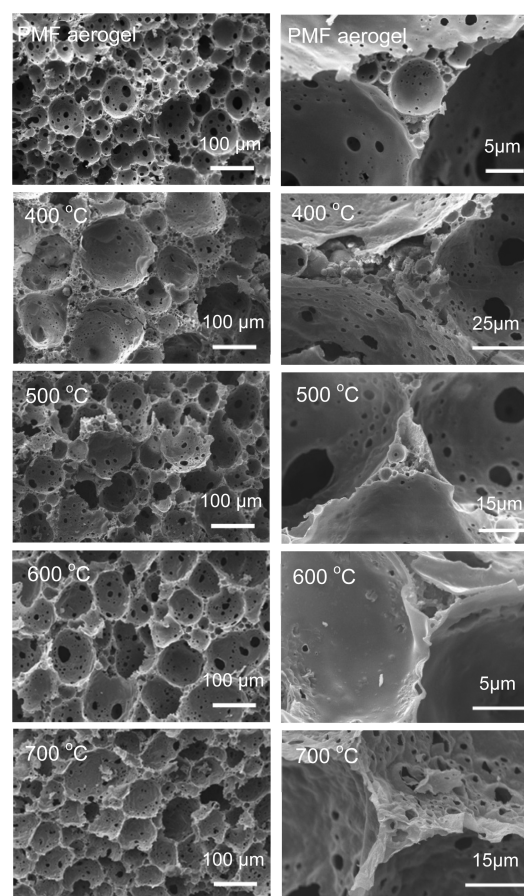


Figure 2. SEM images of the original PMF aerogel and the NRC aerogel prepared by pyrolysis at different temperatures: 400, 500, 600, and 700 $^{\circ}\text{C}$.

absorption of colloidal lignin particles at the oil/water interface. Then, the as-prepared Pickering HIPEs were transferred into an oven at 70 $^{\circ}\text{C}$ for 4 h to polymerizing the pre-MF monomers. PMF aerogels were obtained by removing the inner oil phase by ethanol extraction and drying at room temperature. SEM image of the PMF aerogels (Figure 1c) shows that the materials

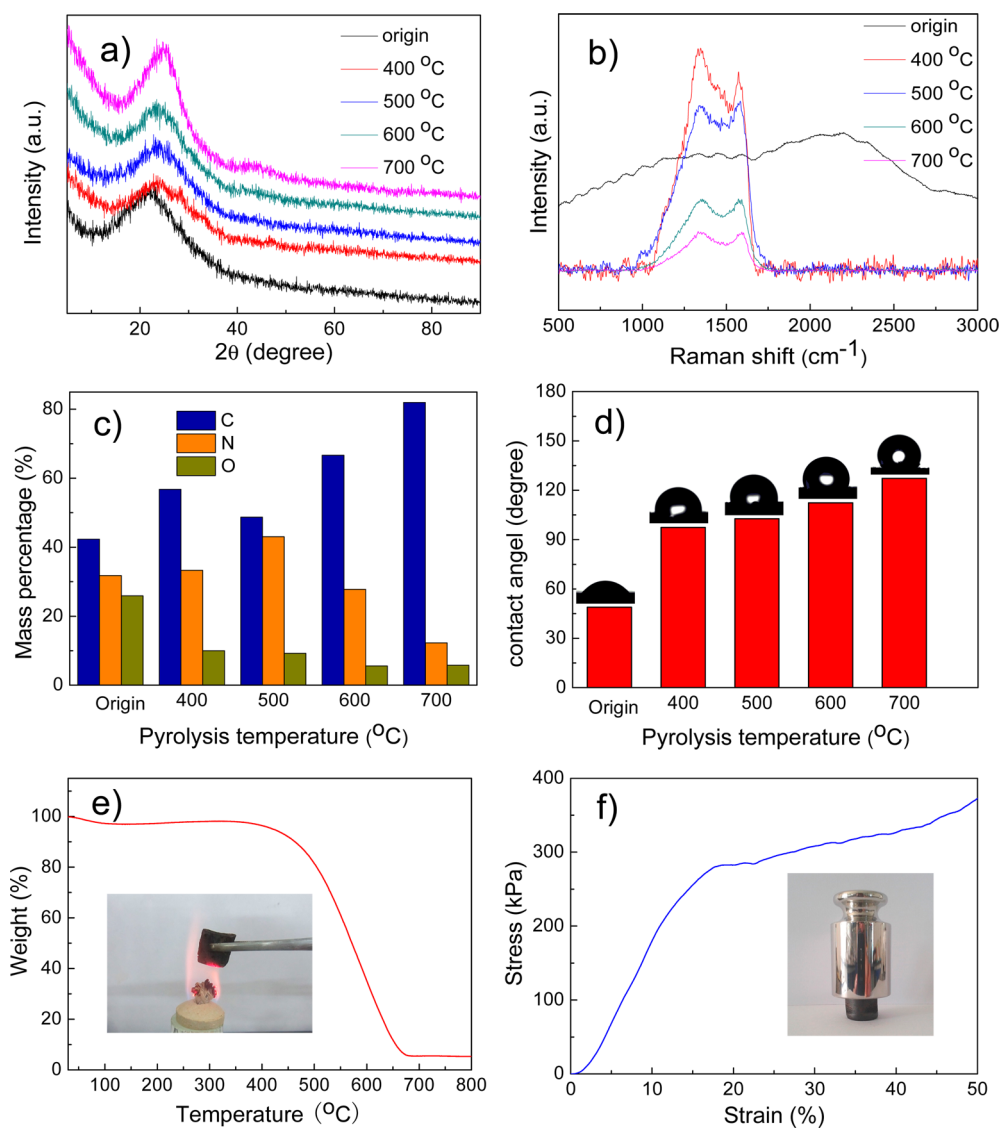


Figure 3. (a) XRD spectra, (b) Raman spectra, (c) element contents, and (d) water contact angle measurements of the original PMF aerogel and the NRC aerogels prepared by pyrolysis at different temperatures. (e) TGA curve of the NRC aerogel that was pyrolyzed at 700 °C. TGA was performed under an air atmosphere and a heating rate of 10 °C min⁻¹ from 30 to 800 °C. The inset in (e) is a photograph of NRC aerogel in a hot flame of an alcohol burner. (f) Typical compression measurements of the fabricated NRC aerogels. The inset in f is a picture of a 200 g weight supported from a 0.13 g NRC aerogel. The weight is more than 1500 times heavier than the monolith.

consist of a well-organized interconnected porous structure of large pore of ca. 100 μm and pore throat of ca. 10 μm. Traced to the Pickering HIPE templates, it can be concluded that the large pores are formed as monomers polymerized only around emulsion droplets and pore throats are formed at the ultrathin contact area between two neighboring droplets. Furthermore, it is interesting to find that the PMF aerogels kept the same volume and shape after the polymerization (see inset pictures in panels b and c in Figure 1), which can be attributed to the excellent stability of the Pickering HIPE templates against any droplet coalescence during the polymerization process. Finally, the NRC aerogels were generated by pyrolyzing the as-prepared PMF aerogels at a high temperature (400–700 °C) under nitrogen atmosphere for 2 h, and thus a high cross-linked carbon structure was obtained. It shows that the NRC aerogels compose of a three-dimensionally interconnected porous structure with macropore of ca. 80 μm and interconnected throat of ca. 5 μm (Figure 1d).

The inner structure is similar to the PMF aerogels even after the pyrolysis process, induced only by a proportional contraction, and it coincided with their macroscale performance (the inset pictures of Figure 1c, d). As the macropore and the interconnecting throat were derived from the initial emulsion droplets, the pore size in principle could be easily tuned by adjusting the internal phase fraction and the pre-MF monomers concentration (see Figure S1 in the Supporting Information).²⁶ The porosity and the surface area of the NRC aerogel fabricated at 700 °C turn out to be 87.7% and 12.51 m²/g respectively, and the average pore size is 3.6 μm (see Figure S2 in the Supporting Information). It is indicated that the lignin particle-stabilized Pickering HIPES are suitable templates to fabricate interconnected porous aerogels.

To create highly cross-linked structure of NRC aerogels, we pyrolyzed PMF aerogels separately at different temperatures. The carbonization treatment and carbonization temperature have a great influence on the final structure of the NRC

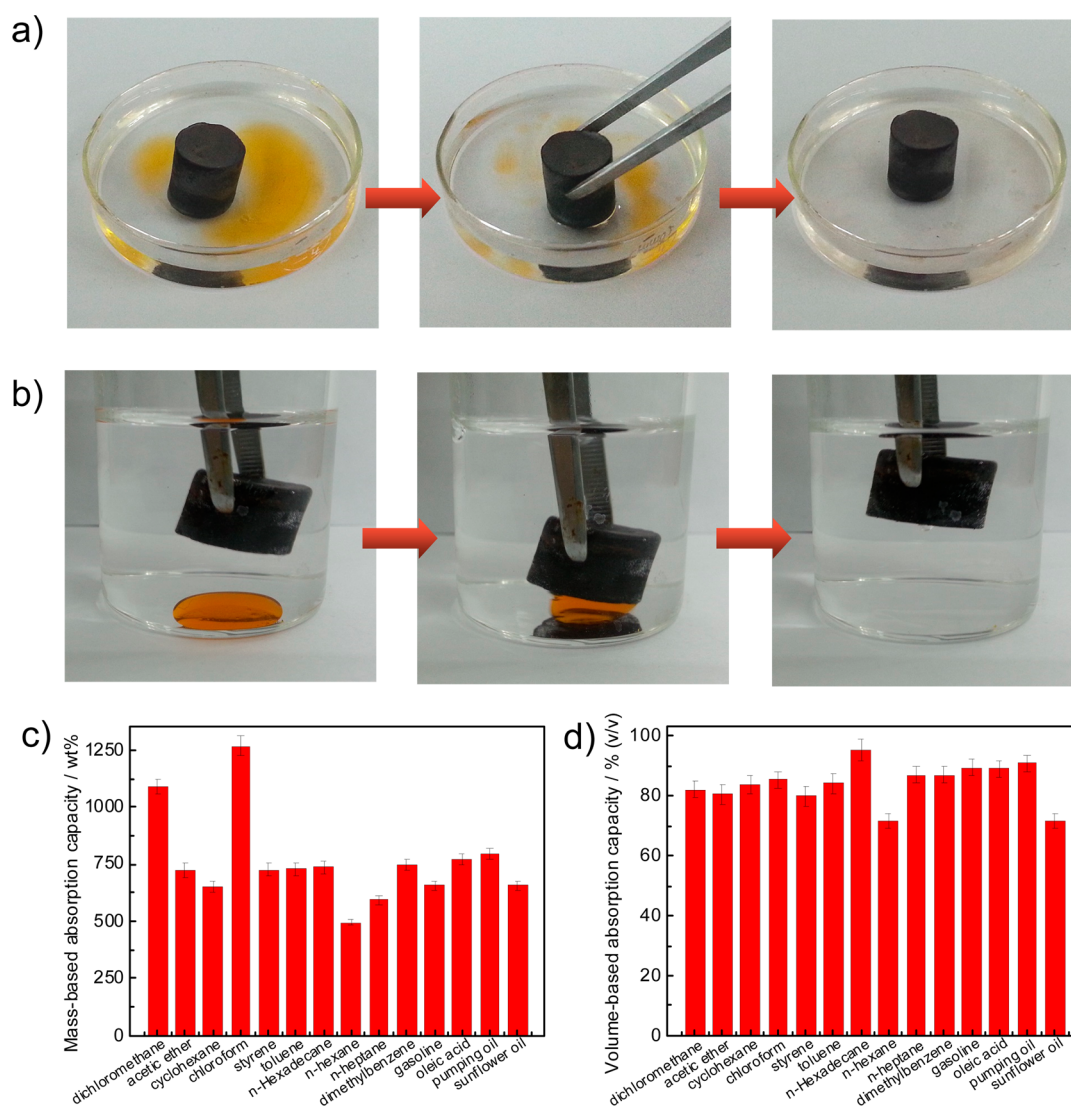


Figure 4. (a) Absorption process of *n*-hexane (stained with Sudan I) floating on water by the NRC aerogel within 5 s. (b) Absorption process of chloroform (stained with Sudan I) at the bottom of water by the NRC aerogel within 3 s. (c) Mass-based and (d) volume-based absorption capacities of the NRC aerogels (with a density of 95 mg cm^{-3}) for oils and nonpolar solvents.

aerogels. From SEM images of Figure 2, one can see that all of the aerogel frameworks maintain an interconnected porous structure, being not clearly affected by the pyrolysis treatment. But the small pores, which exist in the triangular area of neighbouring large pores, disappear gradually with increasing the pyrolysis temperature. And the thickness of the skeleton film became gradual thin with the increasing temperature treatment. Moreover, the increased volume contraction of aerogels as a function of temperature leads to an increase of the aerogel density from 24 to 95 mg cm^{-3} (see Figure S3 in the Supporting Information). X-ray diffraction (XRD) pattern (Figure 3a) shows that the original PMF aerogel is amorphous. While after pyrolysis treatment, a broadened peak centered at 22.5° corresponding to the (002) plane of graphite was observed. There are also two characteristic peaks related to the D and G bands located around 1375 and 1570 cm^{-1} in Raman spectra of Figure 3b, and it is generally accepted that the relative intensity ratio of the D to G bands (I_D/I_G) is the indication of disorder or defects in the carbon structure.⁴² The effect of pyrolysis temperature was also revealed by Fourier transformed infrared (FT-IR) spectra (see Figure S4 in the

Supporting Information), in which the main absorption peaks of functional groups, such as triazine ring, C–O, C–H, and O–H, gradually became weaker and finally disappeared, thereby indicating the improvement of carbonization degree with the elevation of pyrolysis temperature. Moreover, the mass amount of carbon increased from 42.3% to 81.9%, and the oxygen decreased from 25.9% to 5.7% (Figure 3c and Figure S5 in the Supporting Information). The amount of nitrogen, however, fluctuated accordingly and still kept at a high level (12.8% after pyrolysis at 700°C). Nitrogen-rich materials, especially melamine-based materials exhibit excellent fire-resistance. The high content of nitrogen is beneficial to enhance the fire-resistance of the obtained aerogels.^{43,44} The above results reveal that the original PMF molecular structure was destroyed after pyrolysis treatment and carbon-based nitrogen-rich aerogels were generated. At the same time, significant changes happen to the aerogel surface wettability. The original PMF aerogel exhibits surface superhydrophilicity with a contact angle of 48.9° . After pyrolysis treatment, the NRC aerogels became hydrophobic and the contact angle of the NRC aerogels changed from 97.4 to 127.2° with increase in the pyrolysis

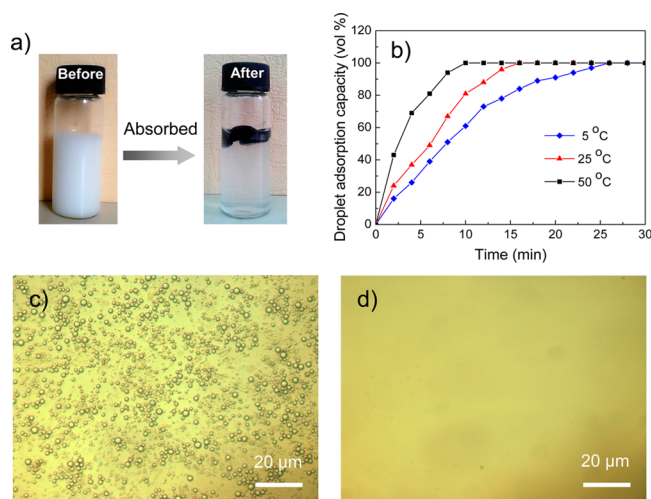


Figure 5. (a) Photographs of toluene-in-water surfactant-free emulsion before and after absorption with NRC aerogel. The emulsion was prepared based on toluene/water volume ratio fixed at 1/10 without any surfactant by ultrasonic. (b) Droplet absorption kinetics of NRC aerogel at 5, 25, and 50 °C. The optical microscopic images of the emulsion (c) before and (d) after absorption with NRC aerogel.

temperatures (Figure 3d). It can be explained that the number of hydrophilic functional groups, such as C=O, C–O, and –OH, gradually decreased with increasing pyrolysis temperature; finally, these groups disappeared, and the nature of the remaining carbon is hydrophobic. By the way, when the pyrolysis temperature is higher than 700 °C, increasing the pyrolysis temperature has no obvious effect on the NRC aerogels wettability (see Figure S6 in the Supporting Information). Therefore, we chose the NRC aerogels pyrolyzed at 700 °C for further study, as they had the highest hydrophobicity and carbonization degree.

The resulted aerogels also exhibit excellent performances in fire-resistant and mechanical behavior. Figure 3e shows the TGA curve of the NRC aerogels performed at air atmosphere. The NRC aerogels reveal to consist of outstanding thermostability as they lost little weight even under 500 °C at air atmosphere, and they exhibit excellent fire-resistant property when exposed to the flame of the alcohol burner without any burning. It is much more enough to suffer the oil combustion in practical oil recovery by an absorption/combustion cycle. Amorphous carbon cannot bear such high temperature at air condition, only graphited carbon can endure harsh terms. For example, when produced single-walled carbon nanotubes in an electric arc discharge, the main by-products are amorphous carbon and graphitic nanoparticles and the purification was conducted by gas phase oxidation of the amorphous carbon in air at 355 °C.⁴⁵ In this work, the pyrolysis temperature is 700 °C, which is far away from the graphitization temperature.²⁷ However, the obtained NRC aerogel can suffer 500 °C in air. This can be ascribed to the abundant nitrogen of the NRC aerogel. Furthermore, the NRC aerogels show excellent mechanical strength. Figure 3f shows plots of compressive stress-strain for the NRC aerogels. Two distinct stages were observed during loading the stress, including an approximate linear elastic region at $\epsilon < 20\%$, followed by a densification region. In the approximate linear elastic region, the compressive stress gradually increased with the strain, composing a compress stress of 282 KPa. In the densification region at $\epsilon > 20\%$, the stress rises slightly with compression, because the

inner honeycomb-like skeleton was gradually destroyed under the compression. Although the NRC aerogels do not have a flexible property as the usual carbon-based aerogels as its special porous structure, but it is because of this that it consists of a much more outstanding mechanical strength for its practical oil clean-up applications.

3.2. Oil and Micrometer-Sized Oil Droplet Absorption Properties. Because of their highly hydrophobic surface, high porosity, and interconnected porous structure, the fabricated NRC aerogels exhibit excellent absorbencies for oils and organic pollutants. Figure 4a shows that when a small piece of NRC aerogel was forced to the *n*-hexane layer (dyed with Sudan I) on a water surface, the oil had been taken up completely in several seconds. Because of its low density and hydrophobicity, the NRC aerogel floated on the water surface after sorption of the *n*-hexane, indicating its potential use for the facile removal of oil spillage and chemical leakage and the ease for recycling. In addition, the NRC aerogels were forced into the water for quick absorption of chloroform (dyed with Sudan I and sink at the bottom of water), and also exhibit quickly oil recovery ability (Figure 4b). The absorption capacity of various kinds of organic solvents and oils was investigated. As the density of the NRC aerogel is 0.095 g cm⁻³, the mass-based absorption capacity is quite low compared with other aerogels with just 6–14 times its own weight (Figure 4c).

As we know, the mass-based absorption capacity is strongly affected by the density of oils and absorbing materials, and in practical use the volume-based absorption capacity ($V_{\text{oil}}/V_{\text{aerogel}}$) is also a very important parameter to characterize the absorptive capability of the absorbents.

$$\begin{aligned}
 V\% &= \frac{V_{\text{oil}}}{V_{\text{absorber}}} \times 100\% \\
 &= \frac{M_{\text{oil}}/\rho_{\text{oil}}}{M_{\text{absorber}}/\rho_{\text{absorber}}} \times 100\% \\
 &= \frac{N_{\text{oil}}\rho_{\text{absorber}}}{\rho_{\text{oil}}} \times 100\% \quad (1)
 \end{aligned}$$

So, we also use volume-based absorption capacity investigate the NRC aerogels oil absorption. As shown in Figure 4d, the volume absorption capacities of the NRC aerogels for oils range from 75.5 to 95.6%, indicating that almost the whole volume of the aerogels is used for oil storage. Compared with other oil absorbents, the NRC aerogel has showed much higher volume-based absorption capacity than many previously reported sorbents, such as ultra-flyweight carbon aerogels (38.1%),¹² Fe₂O₃/C foams (26.7%),²⁵ carbonaceous nanofiber aerogels (22.8%),²³ superhydrophobic and superoleophilic polyurethane sponges (11.5%),²⁴ graphene oxide foams (58.9%),²⁰ and nitrogen-doped graphene frameworks (48.5%).¹⁶ Although the volume-based sorption capacity of NRC aerogel is still lower than that of hydrophobic porous polymethylsilsesquioxane aerogels,²² magnetic carbon nanotube sponges,¹³ graphene-CNT hybrid foams,¹¹ carbon nanotube foams, carbon nanofiber/carbon foam composite⁴⁶ and nanotube-based 3D frameworks,⁴⁷ the production method for NRC aerogel is simple and its precursor materials are conventional industrial resources. The reason for the high oil-absorption capacity is that oils are mainly stored in the pores which were formed on the templates of the HIPE droplets. In this work, the internal phase fraction of the HIPE templates was 85 vol %, and the resulted volume-based sorption capacity of NRC aerogel is also

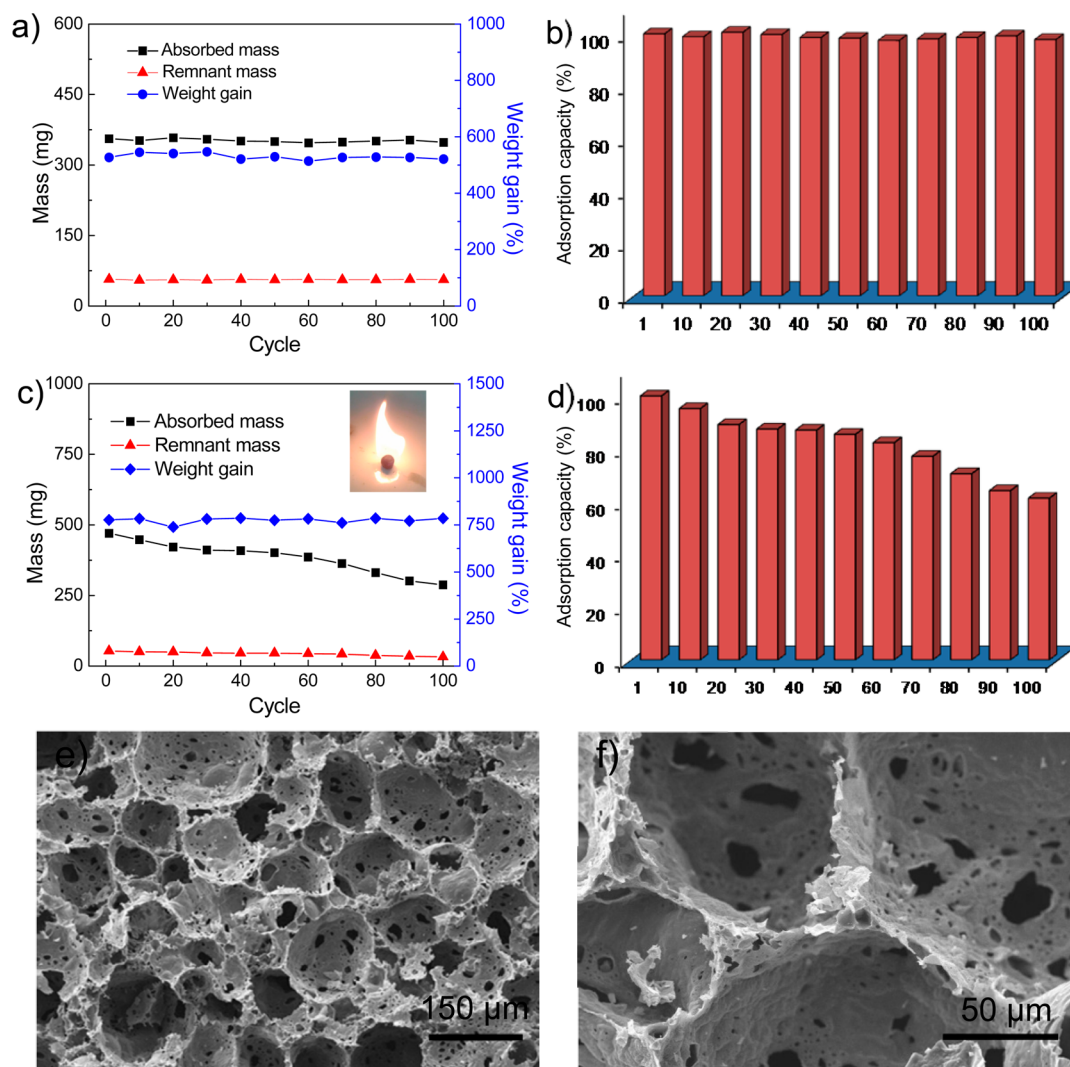


Figure 6. (a, b) Recyclability of NRC aerogels for absorption of *n*-hexane when using the distillation method. (c, d) Recyclability of NRC aerogels for absorption of *n*-hexadecane (with a boiling point of 287 °C) when using the direct combustion method. The inset shows the photograph of burning aerogel saturated with *n*-hexadecane. (e, f) SEM images of the NRC aerogel after 100 absorption/combustion cycles.

around 85%, as the HIPE templates are remarkably stable without any droplet coalescence maintaining the defined pore space for oil storage. Even though the porosity of NRC aerogel is 87.7%, volume-based absorption capacity of some kinds of absorbed oils exhibits larger than the porosity. As shown in Figure 4d, only viscous oils like *n*-hexadecane, oleic acid, pumping oil possess this result. It can be ascribed to the excess viscous oils adhering on the absorbent surface resulting in the volume-based absorption capacity larger than absorbent porosity. It is safe to say that the volume-based volume capacity of the HIPE-templated aerogels is controllable by adjusting the internal phase fraction. Generally, although the present NRC aerogels exhibit a lower mass-based capacity than their ultralight carbonaceous absorbents, they still show one of the most efficient space utilizations for oil absorption.

Furthermore, many micrometer-sized oil droplets were generated in practical marine oil-spill accidents and cannot be effectively absorbed by traditional sorbents, resulting in enormous potential destruction to marine ecosystem. Fortunately, our fabricated NRC aerogels, consisting of double pore structure, namely, large pores (ca. 80 μm) and large pore throats (ca. 5 μm), can capture and absorb the micrometer-sized

oil droplets effectively. To test the oil droplets separation efficiency of the NRC aerogels, a surfactant-free toluene-in-water emulsion was prepared. A piece of NRC aerogels was forced into the emulsion, and the emulsion turned transparent gradually in 15 min at 25 °C (Figure 5). To clearly see an effective separation, optical microscopy was used to observe the difference of original emulsions and their corresponding aerogel-absorbed solution. Figure 5d shows that no droplet exists in the aerogel-absorbed solution in the whole image, indicating the effectiveness of the NRC aerogels for separating oil-in-water emulsions. The absorption kinetics was to establish the time course of oil droplets uptakes on the NRC aerogels (Figure 5b). It took 10 min to achieve absorption equilibrium at 50 °C, which was much faster than 25 °C of 16 min and 5 °C for 26 min. It indicated that with the increasing of the temperature the NRC aerogels have a faster absorption rate of oil droplets. The micrometer-sized oil absorption capacity of the NRC aerogels may mainly because of the hydrophobic skeleton of the materials. Unlike other carbon aerogels, which mostly consisted of nanofibers (nanometer level size) or submicrometer-sheets,^{13–17} these NRC aerogels comprise micrometer-sheets (tens of micrometers). These large hydro-

phobic sheets provide large enough contact area with the oil droplets, resulting in much more time for the oil droplet contacting with the hydrophobic sheet surfaces. In this way, the oil droplets break out and wet the hydrophobic sheet (see Figure S7 in the Supporting Information) and our materials can absorb the micrometer-sized oils. Therefore, the NRC aerogel is an ideal absorbent for the separation of oil and water, especially the absorption of micrometer-sized oil droplets from aqueous phases, which is well beyond what can be achieved by most existing aerogels.

3.3. Absorption Recyclability of NRC Aerogels. The recyclability of the NRC aerogels and the recoverability of pollutants are key criteria for oil/chemical cleanup applications.^{48–52} The regeneration of NRC aerogels is illustrated in Figure 6. Firstly, distillation was employed for recycling (Figure 6a). After absorption, the sample was heated to the boiling point to release the absorbed liquid. Then, we collected the vapour of the liquid for recycling. It is desirable to note that no obvious change in absorption capacity was found after 100 absorption/distillation cycles (Figure 6b). This can be likely attributed to the size and the porous structure, which stayed the same during the whole process. However, in the practical situation, the circulatory way of absorption/distillation can only be applied to repeatedly absorb oils with low boiling point. Other ways should be introduced to circularly recover the high boiling point oils, which cannot be distilled conveniently. Therefore, direct combustion in air was used as an alternative method for recycling (Figure 5c, and Figures S8 and S9 in the Supporting Information). The NRC aerogels were employed for absorbing hexadecane which have a boiling point of 287 °C by an absorption/combustion cycle. It is surprising to find that these NRC aerogels maintain their absorption capacities as high as 61.2% for its original even after 100 absorption/combustion cycles (Figure 5d). The weight gain of every cycle of oil-absorbed NRC aerogels remained unchanged (Figure 5c). Moreover, from the SEM images of the NRC aerogels that were used for 100 absorption/combustion cycles in panels e and f in Figure 5, the porous structure still remained perfectly, only with the skeleton film becoming thinner and resulting in more pore throats, thus making it recyclable for many times. In this way, the spill oils can be transferred to a suitable place avoiding further pollution of the ocean, and can be reused in a energy-recover step. We contribute this excellent fire-resistant property to structure of the resulting materials: Our aerogels are nitrogen-rich, exhibiting a much more outstanding fire-resistant property; in addition, by templating from HIPES, our aerogels consist of carbon film of micro-level, which may be beneficial for fire-resistant and greatly increase the absorption rate and capacity. The results clearly show the excellent recyclability of the NRC aerogel when used as an absorbent.^{53–56}

4. CONCLUSIONS

In summary, we report a facile approach to successfully fabricate the nitrogen-rich carbon aerogel (NRC) with highly hydrophobic surfaces and excellent fire-resistant property. The NRC aerogels were used as oil-sorbent materials to absorb oils or organic solvents in oil-spilled accidents by an absorption/distillation or absorption/combustion ways effectively. It maintained 100% for its initial absorption capacities after 100 absorption/distillation cycles and 61.2% after 100 absorption/combustion cycles. Besides, the NRC aerogels can absorb the micrometer-sized oil droplets which would do inestimable damage to the marine ecosystem. Other potential applications

of the NRC aerogel including 3D electrode materials for lithium-ion batteries, catalyst supports and supercapacitors are expected to be explored in our future works.

■ ASSOCIATED CONTENT

Supporting Information

Characterization of carbon aerogels and oil removal. This material is available free of charge via the Internet at <http://pubs.acs.org>.

■ AUTHOR INFORMATION

Corresponding Authors

*E-mail: zhywang@scut.edu.cn. Tel & Fax: +86-20-22236269

*E-mail: tongai@cuhk.edu.hk. Tel: + 852-39431222. Fax: + 852-26035057.

Author Contributions

The manuscript was written through contributions of all authors. All authors have given approval to the final version of the manuscript.

Funding

National Basic Research Program of China (973 Program, 2012CB821500); National Natural Science Foundation of China (21274046); Natural Science Foundation of Guangdong Province (S20120011057); Hong Kong Special Administration Region (HKSAR) General Research Fund (CUHK403210, 2130237).

Notes

The authors declare no competing financial interest.

■ REFERENCES

- (1) Field, R. W. Separation by Reconfiguration. *Nature* **2012**, *489*, 41–42.
- (2) Yuan, J. K.; Liu, X. G.; Akbulut, O.; Hu, J. Q.; Suib, S. L.; Kong, J.; Stellacci, F. Superwetting Nanowire Membranes for Selective Absorption. *Nat. Nanotechnol.* **2008**, *3*, 332–336.
- (3) Jin, M. H.; Wang, J.; Yao, X.; Liao, M. Y.; Zhao, Y.; Jiang, L. Underwater Oil Capture by A Three-Dimensional Network Architected Organosilane Surface. *Adv. Mater.* **2011**, *23*, 2861–2864.
- (4) Xue, Z. X.; Wang, S. T.; Lin, L.; Cahen, L.; Liu, M. J.; Feng, L.; Jiang, L. A Novel Superhydrophilic and Underwater Superoleophobic Hydrogel-coated Mesh for Oil/Water Separation. *Adv. Mater.* **2011**, *23*, 4270–4273.
- (5) Korhonen, J. T.; Kettunen, M.; Ras, R. H. A.; Ikkala, O. Hydrophobic Nanocellulose Aerogels as Floating, Sustainable, Reusable, and Recyclable Oil Absorbents. *ACS Appl. Mater. Interfaces* **2011**, *3*, 1813–1816.
- (6) Lei, W. W.; Portehault, D.; Liu, D.; Qin, S.; Chen, Y. Porous Boron Nitride Nanosheets for Effective Water Cleaning. *Nat. Commun.* **2013**, *4*, 1777.
- (7) Kota, A. K.; Kwon, G.; Choi, W.; Mabry, J. M.; Tuteja, A. Hygro-responsive Membranes for Effective Oil-Water Separation. *Nat. Commun.* **2012**, *3*, 1025.
- (8) Kwon, G.; Kota, A. K.; Li, Y. X.; Sohani, A.; Mabry, J. M.; Tuteja, A. On-demand Separation of Oil-Water Mixtures. *Adv. Mater.* **2012**, *24*, 3666–3671.
- (9) Li, K.; Ju, J.; Xue, Z. X.; Ma, J.; Feng, L.; Gao, S.; Jiang, L. Structured Cone Arrays for Continuous and Effective Collection of Micron-sized Oil Droplets from Water. *Nat. Commun.* **2013**, *4*, 1038.
- (10) Chu, Y.; Pan, Q. M. Three-dimensionally Macroporous Fe/C Nanocomposites as Highly Selective Oil-absorption Materials. *ACS Appl. Mater. Interfaces* **2012**, *4*, 2420–2425.
- (11) Dong, X. C.; Chen, J.; Ma, Y. W.; Wang, J.; Chan-Park, M. B.; Liu, X. M.; Wang, L. H.; Huang, W.; Chen, P. Superhydrophobic and Superoleophilic Hybrid Foam of Graphene and Carbon Nanotube for

Selective Removal of Oils or Organic Solvents from the Surface of Water. *Chem. Commun.* **2012**, 48, 10660–10662.

(12) Sun, H. Y.; Xu, Z.; Gao, C. Multifunctional, Ultra-flyweight, Synergistically Assembled Carbon Aerogels. *Adv. Mater.* **2013**, 25, 2554–2560.

(13) Gui, X. C.; Zeng, Z. P.; Lin, Z. Q.; Gan, Q. M.; Xiang, R.; Zhu, Y.; Cao, A. Y.; Tang, Z. K. Magnetic and Highly Recyclable Macroporous Carbon Nanotubes for Spilled Oil Sorption and Separation. *ACS Appl. Mater. Interfaces* **2013**, 5, 5845–5850.

(14) Calcagnile, P.; Fragouli, D.; Bayer, I. S.; Anyfantis, G. C.; Martiradonna, L.; Cozzoli, P. D.; Cingolani, R.; Athanassiou, A. Magnetically Driven Floating Foams for the Removal of Oil Contaminants from Water. *ACS Nano* **2012**, 6, 5413–5419.

(15) Nguyen, D. D.; Tai, N. H.; Lee, S. B.; Kuo, W. S. Superhydrophobic and Superoleophilic Properties of Graphene-based Sponges Fabricated Using a Facile Dip Coating Method. *Energy Environ. Sci.* **2012**, 5, 7908–7912.

(16) Zhao, Y.; Hu, C. G.; Hu, Y.; Cheng, H. H.; Shi, Q.; Lu, L. T. A Versatile, Ultralight, Nitrogen-doped Graphene Framework. *Angew. Chem. Int. Ed.* **2012**, 51, 11371–11375.

(17) Men, Y. J.; Siebenbürger, M.; Qiu, X. L.; Antonietti, M.; Yuan, J. Y. Low Fractions of Ionic Liquid or Poly(ionic liquid) can Activate Polysaccharide Biomass into Shaped, Flexible and Fire-retardant Porous Carbons. *J. Mater. Chem. A* **2013**, 1, 11887–11893.

(18) Cong, H.P.; Ren, X.C.; Wang, P.; Yu, S.H. Macroscopic Multifunctional Graphene-based Hydrogels and Aerogels by a Metal Ion Induced Self-assembly Process. *ACS Nano* **2012**, 6, 2693–2703.

(19) Gui, X. C.; Wei, J. Q.; Wang, K. L.; Cao, A. Y.; Zhu, H. W.; Jia, Y.; Shu, Q. K.; Wu, D. H. Carbon Nanotube Sponges. *Adv. Mater.* **2010**, 22, 617–621.

(20) Niu, Z. Q.; Chen, J.; Hng, H. H.; Ma, J.; Chen, X. D. A Leavening Strategy to Prepare Reduced Graphene Oxide Foams. *Adv. Mater.* **2012**, 24, 4144–4150.

(21) Bi, H. C.; Xie, X.; Yin, K. B.; Zhou, Y. L.; Wan, S.; He, L. B.; Xu, F.; Banhart, F.; Sun, L. T.; Ruoff, R. S. Spongy Graphene as a Highly Efficient and Recyclable Sorbent for Oils and Organic Solvents. *Adv. Funct. Mater.* **2012**, 22, 4421–4425.

(22) Hayase, G.; Kanamori, K.; Fukuchi, M.; Kaji, H.; Nakanishi, K. Facile Synthesis of Marshmallow-like Macroporous Gels Usable under Harsh Conditions for the Separation of Oil and Water. *Angew. Chem., Int. Ed.* **2013**, 52, 1986–1989.

(23) Liang, H. W.; Guan, Q. F.; Chen, L. F.; Zhu, Z.; Zhang, W. J.; Yu, S. H. Macroscopic-scale Template Synthesis of Robust Carbonaceous Nanofiber Hydrogels and Aerogels and Their Applications. *Angew. Chem., Int. Ed.* **2012**, 51, 5101–5105.

(24) Zhu, Q.; Pan, Q. M.; Liu, F. T. Facile Removal and Collection of Oils from Water Surfaces through Superhydrophobic and Superoleophilic Sponges. *J. Phys. Chem. C* **2011**, 115, 17464–17470.

(25) Chen, N.; Pan, Q. M. Versatile Fabrication of Ultralight Magnetic Foams and Application for Oil-Water Separation. *ACS Nano* **2013**, 8, 6875–6883.

(26) Wei, G.; Miao, Y.; Zhang, C.; Yang, Z.; Liu, Z. Y.; Tjui, W. W.; Liu, T. X. Ni-doped Graphene/Carbon Cryogels and Their Applications As Versatile Sorbents for Water Purification. *ACS Appl. Mater. Interfaces* **2013**, 5, 7584–7591.

(27) Wu, Z. Y.; Li, C.; Liang, H. W.; Chen, J. F.; Yu, S. H. Ultralight, Flexible, and Fire-Resistant Carbon Nanofiber Aerogels from Bacterial Cellulose. *Angew. Chem., Int. Ed.* **2013**, 52, 2925–2929.

(28) Bi, H. C.; Yin, Z. Y.; Cao, X. H.; Xie, X.; Tan, C. L.; Huang, X.; Chen, B.; Chen, F. T.; Yang, Q. L.; Bu, X. Y.; Lu, X. H.; Sun, L. T.; Zhang, H. Carbon Fiber Aerogel Made from Raw Cotton: A Novel, Efficient and Recyclable Sorbent for Oils and Organic Solvents. *Adv. Mater.* **2013**, 25, 5916–5921.

(29) Johnson, D. W.; Sherborne, C.; Didsbury, M. P.; Pateman, C.; Cameron, N. R.; Clayssens, F. Macrostructuring of Emulsion-templated Porous Polymers by 3D Laser Patterning. *Adv. Mater.* **2013**, 25, 3178–3181.

(30) Chen, Y. H.; Ballard, N.; Bon, S. A. F. Moldable High Internal Phase Emulsion Hydrogel Objects from Non-Covalently Crosslinked

Poly(N-isopropylacrylamide) Nanogel Dispersions. *Chem. Commun.* **2013**, 49, 1524–1526.

(31) Sun, G. Q.; Li, Z. F.; Ngai, T. Inversion of Particle-stabilized Emulsions to Form High Internal Phase Emulsions. *Angew. Chem. Int. Ed.* **2010**, 49, 2163–2166.

(32) Yang, Y.; Wei, Z. J.; Wang, C. Y.; Tong, Z. Lignin-based Pickering HIPEs for Macroporous Foams and Their Enhanced Adsorption of Copper (II) Ions. *Chem. Commun.* **2013**, 49, 7144–7146.

(33) Ning, Y.; Yang, Y.; Wang, C. Y.; Ngai, T.; Tong, Z. Hierarchical Porous Polymeric Microspheres as Efficient Adsorbents and Catalyst Scaffolds. *Chem. Commun.* **2013**, 49, 8761–8763.

(34) Yang, Y.; Wei, Z. J.; Wang, C. Y.; Tong, Z. Versatile Fabrication of Nanocomposite Microcapsules with Controlled Shell Thickness and Low Permeability. *ACS Appl. Mater. Interfaces* **2013**, 5, 2495–2502.

(35) Ning, Y.; Wang, C. Y.; Ngai, T.; Tong, Z. Fabrication of Tunable Janus Microspheres with Dual Anisotropy of Porosity and Magnetism. *Langmuir* **2013**, 29, 5138–5144.

(36) Wei, Z. J.; Yang, Y.; Yang, R.; Wang, C. Y. Alkaline Lignin Extracted from Furfural Residues for pH-responsive Pickering Emulsions and Their Recyclable Polymerization. *Green Chem.* **2012**, 14, 3230–3236.

(37) Thompson, K. L.; Chambon, P.; Verber, R.; Armes, S. P. Can Polymersomes Form Colloidosomes? *J. Am. Chem. Soc.* **2012**, 134, 12450–12453.

(38) Oschatz, M.; Borchardt, L.; Thommes, M.; Cychosz, K. A.; Senkovska, I.; Klein, N.; Frind, R.; Leistner, M.; Presser, V.; Gogotsi, Y.; Kaskel, S. Carbide-derived Carbon Monoliths with Hierarchical Pore Architectures. *Angew. Chem., Int. Ed.* **2012**, 51, 7577–7580.

(39) Li, T. T.; Liu, H. R.; Zeng, L.; Yang, S.; Li, Z. C.; Zhang, J. D.; Zhou, X. T. Macroporous Magnetic Poly(styrene-divinylbenzene) Nanocomposites Prepared via Magnetite Nanoparticles-stabilized High Internal Phase Emulsions. *J. Mater. Chem.* **2011**, 21, 12865–12872.

(40) Zheng, Z.; Zheng, X. H.; Wang, H. T.; Du, Q. G. Macroporous Graphene Oxide–Polymer Composite Prepared through Pickering High Internal Phase Emulsions. *ACS Appl. Mater. Interfaces* **2013**, 5, 7974–7982.

(41) Ikem, V. O.; Menner, A.; Horozov, T. S.; Bismarck, A. Highly Permeable Macroporous Polymers Synthesized from Pickering Medium and High Internal Phase Emulsion Templates. *Adv. Mater.* **2010**, 22, 3588–3592.

(42) Chen, L. F.; Huang, Z. H.; Liang, H. W.; Yao, W. T.; Yu, Z. Y.; Yu, S. H. Flexible All-Solid-State High-Power Supercapacitor Fabricated with Nitrogen-doped Carbon Nanofiber Electrode Material Derived from Bacterial Cellulose. *Energy Environ. Sci.* **2013**, 6, 3331–3338.

(43) Wang, Q.; Chen, Y. H.; Liu, Y.; Yin, H.; Aelmans, N.; Kierkels, R. Performance of an Intumescent-flame-retardant Mater Batch Synthesized by Twin-screw Reactive Extrusion: Effect of the Polypropylene Carrier Resin. *Polym. Int.* **2004**, 53, 439–448.

(44) Wang, Z. Y.; Han, E. H.; Ke, W. Influence of Nano-LDHs on Char Formation and Fire-resistant Properties of Flame-retardant coating. *Prog. Org. Coat.* **2005**, 53, 29–37.

(45) Gajewski, S.; Maneck, H. E.; Knoll, U.; Neubert, D.; Dörfel, I.; Mach, R.; Strauß, B.; Friedrich, J. F. Purification of Single Walled Carbon Nanotubes by Thermal Gas Phase Oxidation. *Diamond Relat. Mater.* **2003**, 12, 816–820.

(46) Xiao, N.; Zhou, Y.; Ling, Z.; Qiu, J. S. Synthesis of a Carbon Nanofiber/Carbon Foam Composite From Coal Liquefaction Residue for the Separation of Oil and Water. *Carbon* **2013**, 59, 530–536.

(47) Hashim, D. P.; Narayanan, N. T.; Romo-Herrera, J. M.; Cullen, D. A.; Hahm, M. G.; Lezzi, P.; Suttle, J. R.; Kelkhoff, D.; Muñoz-Sandoval, E.; Ganguli, S.; Roy, A. K.; Smith, D. J.; Vajtai, R.; Sumpter, B. G.; Meunier, V.; Terrones, H.; Terrones, M.; Ajayan, P. M. Covalently Bonded Three-dimensional Carbon Nanotube Solids via Boron Induced Nanojunctions. *Sci. Rep.* **2012**, 2, 363.

(48) Jing, P.; Fang, X. H.; Yan, J. L.; Guo, J.; Fang, Y. Ultra-low Density Porous Polystyrene Monolith: Facile Preparation and Superior Application. *J. Mater. Chem. A* **2013**, *1*, 10135–10141.

(49) Zhang, A. J.; Chen, M. J.; Du, C.; Guo, H. Z.; Bai, H.; Li, L. Poly(dimethylsiloxane) Oil Absorbent with a Three-dimensionally Interconnected Porous Structure and Swellable Skeleton. *ACS Appl. Mater. Interfaces* **2013**, *5*, 10201–10206.

(50) Sai, H. Z.; Xing, L.; Xiang, J. H.; Cui, L. J.; Jiao, J. B.; Zhao, C. L.; Li, Z. Y.; Li, F. Flexible Aerogels Based on an Interpenetrating Network of Bacterial Cellulose and Silica by a Non-supercritical Drying Process. *J. Mater. Chem. A* **2013**, *1*, 7963–7970.

(51) Liu, Y. F.; Ba, H.; Nguyen, D. L.; Ersen, O.; Romero, T.; Zafeiratos, S.; Begin, D.; Janowska, I.; Pham-Huu, C. Synthesis of Porous Carbon Nanotubes Foam Composites with a High Accessible Surface Area and Tunable Porosity. *J. Mater. Chem. A* **2013**, *1*, 9508–9516.

(52) Hu, Y.; Liu, X. Y.; Zou, J. C.; Gu, T.; Chai, W. B.; Li, H. B. Graphite/Isobutylene-isoprene Rubber Highly Porous Cryogels as New Sorbents for Oil Spills and Organic Liquids. *ACS Appl. Mater. Interfaces* **2013**, *5*, 7737–7742.

(53) Zhu, Q.; Chu, Y.; Wang, Z. K.; Chen, N.; Lin, L.; Liu, F. T.; Pan, Q. M. Robust Superhydrophobic Polyurethane Sponge as a Highly Reusable Oil-absorption Material. *J. Mater. Chem. A* **2013**, *1*, 5386–5393.

(54) Liu, Y.; Ma, J. K.; Wu, T.; Wang, X. R.; Huang, G. B.; Liu, Y.; Qiu, H. X.; Li, Y.; Wang, W.; Gao, J. P. Cost-effective Reduced Graphene Oxide-coated Polyurethane Sponge As a Highly Efficient and Reusable Oil-absorbent. *ACS Appl. Mater. Interfaces* **2013**, *5*, 10018–10026.

(55) Li, R.; Chen, C. B.; Li, J.; Xu, L. M.; Xiao, G. Y.; Yan, D. Y. A Facile Approach to Superhydrophobic and Superoleophilic Graphene/Polymer Aerogels. *J. Mater. Chem. A* **2014**, *2*, 3057–3064.

(56) Wang, C. F.; Lin, S. L. Robust Superhydrophobic/Superoleophilic Sponge for Effective Continuous Absorption and Expulsion of Oil Pollutants from Water. *ACS Appl. Mater. Interfaces* **2013**, *5*, 8861–8864.